Published in final edited form as:
Cytometry A. 2009 October ; 75(10): 840–847. doi:10.1002/cyto.a.20778.

DNA Damage Response Induced by Tobacco Smoke in Normal Human Bronchial Epithelial and A549 Pulmonary Adenocarcinoma Cells Assessed by Laser Scanning Cytometry

Hong Zhao[1], **Anthony P. Albino**[1,2], **Ellen Jorgensen**[1,2], **Frank Traganos**[1], and **Zbigniew Darzynkiewicz**[1]

[1]New York Medical College, Valhalla, NY, 10595

[2]Vector Research LLC. 712 Fifth Ave. New York, NY 10019

Abstract

Cigarettes smoke (CS) is a major cause of lung cancer and a contributor to the development of a wide range of other malignancies. There is an acute need to develop a methodology that can rapidly assess the potential carcinogenic properties of the genotoxic agents present in CS. We recently reported that exposure of normal human bronchial epithelial cells (NHBE) or A549 pulmonary carcinoma cells to CS induces activation of ATM through its phosphorylation on *Ser*1981 and phosphorylation of histone H2AX on *Ser139* (γH2AX) most likely in response to formation of the potentially carcinogenic DNA double-strand breaks (DSBs). To obtain a more complete view of the DNA damage response (DDR) we explored the correlation between ATM activation, H2AX phosphorylation, activation of Chk2 through its phosphorylation on *Thr*68 and phosphorylation of p53 on *Ser*15 in NHBE and A549 cell exposed to CS. Multiparameter analysis by laser scanning cytometry made it possible to relate these DDR events, detected immunocytochemically, with cell cycle phase. The CS-dose dependent induction and increase in the extent of phosphorylation of ATM, Chk2, H2AX and p53 were seen in both cell types. ATM and Chk2 were phosphorylated ~ 1 h prior to phosphorylation of H2AX and p53. Dephosphorylation of ATM, Chk2 and H2AX was seen after 2h following CS exposure. The dose-dependency and kinetics of DDR was essentially similar in both cell types which provides justification for the of use A549 cells in assessment of genotoxicity of CS in lieu of normal bronchial epithelial cells. The observation that DDR was more pronounced in S-phase cells is consistent with the mechanism of induction of DSBs occurring as a result of collision of replication forks with primary lesions such as DNA adducts that can be caused by CS-generated oxidants. Cytometric assessment of CS-induced DDR provides a means to estimate the genotoxicity of CS and to explore the mechanisms of the response as a function of cell cycle phase and cell type.

Keywords

ATM activation; histone H2AX phosphorylation; gammaH2AX; Chk2 activation; Ser15 p53 phosphorylation; checkpoint; laser scanning cytometry; cell cycle

Corresponding author: Dr. Z. Darzynkiewicz, Brander Cancer Research Institute at NYMC, Department of Pathology, BSB 438, Valhalla, NY 10595, Tel: 914-594-3780, Fax: 914-594-3790, darzynk@nymc.edu.

Introduction

Cigarette smoke (CS) is not only the major cause of lung cancer, but also contributes to the development of other malignancies such as oral, pharynx, larynx, esophagus, bladder, stomach, kidney, pancreas and uterine cervix cancers as well as myeloid leukemias (reviews, 1–5). Nuclear DNA is the target of a number of genotoxic agents of different chemical structure present in CS. During the past several decades extensive studies have been carried out to: (i) identify the genotoxic agents present it CS; (ii) define the types of DNA lesions induced by these agents, and (iii) characterize mechanisms by which these lesions lead to cancer development. A vast literature exists indicating the exceedingly complex genotoxic impact of CS. Over 60 carcinogens collectively defined as the “Hoffman list” were identified in CS (6–8). Among them are potent carcinogenic constituents such as polycyclic aromatic hydrocarbons, in particular benzo(a)pyrene (BaP), and tobacco-specific nitrosamines such as NNK [4- (methylnitrosamino)-1-(3-pyridyl)-1-butanone] and NNN (N'-nitrosonornicotine) (1–3) (1,4–13). The DNA lesions induced by genotoxins in CS considered the tobacco carcinogen biomarkers include the DNA adducts of BaP, tobacco-specific nitrosamines, alkylating agents, aldehydes and other lipid peroxidation products, and products of oxidative damage such as 8-oxo-dGuo (review, 8). These DNA lesions collectively cause accumulation of genetic defects at multiple loci (1,4–12) which leads to progressive genomic damage and instability (14–17). The tumorigenic relevance of this damage and instability is revealed by studies indicating that smokers with less efficient DNA repair capacities are at higher risk for developing lung cancer (18–20). Thus, defining the temporal sequence of molecular responses to CS-induced genetic damage can clarify the types of DNA damage that play a contributory role in carcinogenesis and provide viable biomarkers of cancer risk in exposed individuals (6,21–24).

We have recently reported that exposure of normal human bronchial epithelial (NHBE) or pulmonary carcinoma A549 cells to CS triggers their histone H2AX phosphorylation on *Ser*139 (so modified H2AX is termed γH2AX) concurrently with activation of ATM through its phosphorylation on *Ser*1981(25–27). Both these events were detected immunocytochemically using phospho-specific γH2AX and ATM-*Ser*1981^{P} Abs, and measured by laser scanning cytometry (LSC). These findings strongly suggested that CS induces DNA lesions and some of these lesions are potentially carcinogenic DNA double-strand breaks (DSBs). The cytometric assessment of H2AX phosphorylation and ATM activation in the cells exposed *in vitro* to CS provided a means to rapidly estimate the genotoxic properties of whole smoke as well as its subclasses of genotoxic constituents.

Activation of ATM and phosphorylation of H2AX are only a part of the mammalian DNA damage response (DDR). Upon induction of damage to DNA, a complex series of events defined as DDR occurs in nuclear chromatin that involve induction of a plethora of molecular interactions between numerous molecules of the DDR machinery. The function of the DDR is to arrest cell cycle progression and division to prevent transfer of DNA damage to progeny cells, to engage the DNA damage repair mechanisms and to activate the apoptotic pathway in order to eliminate cells with excessive DNA damage that cannot be repaired (reviews, 28–34).

We have recently adopted other immunocytochemical markers of DDR, namely the phosphorylation of Chk2 on *Thr*68 and phosphorylation of tumor suppressor p53 on *Ser*15 as cytometric probes to further explore mechanisms of DDR in relation to cell cycle phase and induction of apoptosis (35–38). In the present study we applied these markers together with the markers of ATM activation and H2AX phosphorylation to investigate DDR in NHBE and in pulmonary adenocarcinoma A549 cells exposed to CS.

Materials and Methods

Cells

NHBE cells were purchased from Cambrex Corporation, East Rutherford, NJ. The cells were cultured in complete Bronchial Epithelial Cell Growth Medium (BEGM) supplemented with retinoic acid, human epidermal growth factor, epinephrine, transferrin, triiodothyronine, insulin, hydrocortisone, bovine pituitary extract and gentamicin by addition of SingleQuots,™ (both medium and the supplements were purchased from Cambrex Corporation, East Rutherford, NJ). Dual-chambered slides (Nunc Lab-Tek II, Fisher Scientific, Pittsburgh, PA) were seeded with 1 ml of a cell suspension containing 8×10^4 cells per chamber. A549 cells were purchased from American Type Culture Collection (ATCC #CCL-185, Manassas, VA). The cells were cultured in Ham's F12K medium with 2mM L-glutamine adjusted to contain 1.5 g/L sodium bicarbonate (ATCC) and supplemented with 10% fetal bovine serum (ATCC). All incubations were at 37° C in a humidified atmosphere of 5% CO_2 in air. Cells were grown to 50% confluency prior to exposure to CS. The cell culture medium was replaced with 37° C Dulbecco's PBS (D-PBS) containing calcium and magnesium (Sigma Chemical Co., St. Louis, MO) for the smoke exposure.

CS exposure

Slide chamber covers were removed and the slides containing cells were placed in a smoke exposure chamber of 20.6 cm length × 6.7 cm width × 6.3 cm height. Smoke was generated from 2R4F (Industry Standard #16, Philip-Morris, Richmond VA) cigarettes under FTC smoking conditions using a KC 5 Port Smoker (KC Automation, Richmond, VA) as described before (25–27). The smoke was diluted by drawing it through a 250 ml round-bottom flask prior to its reaching the exposure chamber. The time and distance that the smoke traveled from the end of the cigarette to the exposure chamber was minimized by using the shortest lengths of tubing possible between the parts of the apparatus. Cigarettes were smoked to within 3 mm of the filter tip. Cells were exposed to smoke for up to 20 minutes. Mock-exposed (control) cells were treated identically for 20 min as the smoke exposed cells except for the absence of a cigarette in the smoking port. Following treatment or mock treatment, the D-PBS was aspirated and replaced with 1 ml per chamber of the fresh respective culture medium at 37 °C. The slides were placed in a 37 °C, 5% CO_2 incubator and incubated for up to 4 h. At the end of the incubation, medium from each chamber was carefully aspirated and 1 ml of 1% fresh methanol-free formaldehyde in 1× D-PBS was added to each chamber and the cells fixed by gently rocking the slides at room temperature for 15 minutes. Following aspiration of the fixative, the chamber slides were disassembled and the slides submerged in 50 ml conical tubes filled with 70% ethanol. The fixed slides were stored at 4 °C prior to analysis.

Immunocytochemical detection of phosphorylated histone H2AX (γH2AX) and activated ATM, Chk2 and p53

After fixation, the cells were then washed twice in PBS and treated on slides with 0.1% Triton X-100 (Sigma) in PBS for 15 min, and then in a 1% (w/v) solution of bovine serum albumin (BSA; Sigma) in PBS for 30 min to suppress nonspecific antibody (Ab) binding. The cells were then incubated in a 100 μl volume of 1% BSA containing 1:200 dilution of phospho-specific (*Ser*139) γH2AX mAb (Biolegend, San Diego, CA) and 1:100 diluted phospho-specific (*Ser*15) p53 rabbit polyclonal Ab (Cell Signaling, Danvers, MA) or 1:100 dilution of phospho-specific (*Ser*1981) ATM mAb (Cell Signaling), and 1:100 diluted phospho-specific (*Thr* 68) Chk2 rabbit polyclonal Ab (Cell Signaling) for 1.5 h at room temperature or overnight at 4° C. The secondary fluorochrome-tagged Abs were either Alexa Fluor 488 tagged Ab (Invitrogen/Molecular Probes, Eugene, OR) at 1;100 dilution

(ATM or γH2AX) or Alexa Fluor 633 Ab (Invitrogen/Molecular Probes, at 1:100 dilution) (Chk2 or p53). Prior to measurement by LSC, the cells were counterstained with 2.8 μg/ml 4,6-diamidino-2- phenylindole (DAPI; Sigma) in PBS for 15 min. Each experiment was performed with an IgG control in which cells were labeled only with secondary antibody, Alexa Fluor 488 goat anti-mouse IgG (H+L) or Alexa Fluor 633 goat anti-rabbit IgG (H+L) without primary antibody incubation, to estimate the extent of nonspecific binding of the secondary antibody to the cells. Other details of cell incubations with the primary and secondary Ab were presented before (35–38).

Measurement of cell fluorescence by LSC

Cellular green or far red IF representing binding of the respective phospho-specific Abs and the blue emission of DAPI stained DNA was measured using an LSC (iCys; CompuCyte, Cambridge, MA) utilizing standard filter settings; Alexa Fluor 488 fluorescence was excited with 488-nm argon, Alexa Fluor 633 fluorescence with a 633 nm helium-neon and DAPI fluorescence with a 405 nm violet laser. The intensities of maximal pixel and integrated fluorescence were measured and recorded for each cell as described (39,40). At least 3,000 cells were measured per sample. Gating analysis was carried out to obtain mean values (± SD) of the intensity of immunofluorescence (IF) of ATM-*Ser*1981^{P}, Chk2-*Thr*68^{P}, γH2AX or p53*Ser*15^{P} of cell populations in G_1 (DNA Index; DI = 0.9 –1.1), S (DI = 1.2 – 1.8) and G_2M (DI = 1.9 – 2.1) phases of the cell cycle in each experiment. The SD was estimated based on Poisson distribution of cell populations. Each experiment was run at least in duplicate, some experiments were additionally repeated. The inter-sample variation in the duplicates and in repeated samples did not exceed the value of two standard deviations of individual samples.

Results

Fig. 1 illustrates the changes in expression of ATM-*Ser*1981^{P}, Chk2-*Thr*68^{P}, γH2AX and p53-*Ser*15^{P} in A549 cells exposed for 15 min to CS and then cultured for 1 h. As is evident CS treatment induced activation of ATM concurrent with activation of Chk2 and phosphorylation of H2AX. These changes appeared more pronounced in S than in G_1 or G_2M phase cells. No distinct changes in expression of p53-*Ser*15^{P} were apparent 1 h after 15-min exposure to CS.

Similar to that observed in A459 cells, exposure of NHBE cells CS also led to phosphorylation of ATM, Chk2 and H2AX and had little effect on phosphorylation of p53 (Fig. 2). Consistent with our earlier observations (25,26,41) non-CS-exposed (mock-treated) NHBE cells expressed γH2AX at a relatively high level, particularly during S phase. The CS-induced increase in expression of γH2AX was most pronounced during the early portion of S phase whereas the increase in phosphorylation of ATM or Chk2 showed no distinct preference to any phase of the cell cycle.

The effect of duration of exposure to CS on the level of induction of ATM-*Ser*1981^{P}, Chk2-*Thr*68^{P}, γH2AX and p53-*Ser*15^{P} in A549 or NHBE cells is presented in Fig. 3. The response to the CS treatment was strikingly similar for both A459 and NHBE cells. Thus, exposure to CS for the initial 5 min had relatively little effect on phosphorylation of ATM, Chk 2 or H2AX in both cell types. However, nearly linear dependence in the extent of phosphorylation of ATM, Chk2 and H2AX vis-à-vis time of exposure to CS was seen in the A549 and NHBE cells exposed for time intervals from 5 to 20 min. The 20 min exposure to CS of both A549 and NHBE cells resulted in approximately a 4-fold increase in the level of phosphorylated ATM (Δ ATM-*Ser*1981^{P}) over the respective controls (mock treated cells; Δ = 1.0). The CS-induced increase in expression of phosphorylated Chk2 in A549 and NHBE cells was also similar, with Δ Chk2-*Thr*68^{P} ranging between 2.5 and 3.0. Phosphorylation of

H2AX induced by treatment with CS, however, was more pronounced in A549 than NHBE cells. As is evident in Fig. 3, after 20 min exposure to CS the Δ γH2AX of A549 was approximately twice higher (4.5 – 5.5) than that of NHBE (2.0–3.0) (Fig. 3). Compared with phosphorylation of ATM, Chk2 or H2AX the CS-induced increase in phosphorylation of p53 was much less distinct with Δ p53-*Ser*15^{P} reaching only 1.5 (50% rise). Phosphorylation of ATM, Chk2 and H2AX in S-phase cells, particularly after 10 and 15 min exposure to CS, was more pronounced than in G_1 or G_2M cells. An exception was H2AX phosphorylation in NHBE cells which was the most extensive in G_1 cells.

The data showing the *kinetics* of DDR in terms of a change in the level of phosphorylation of ATM, Chk2, H2AX and p53 in cells exposed to CS for 20 min and then cultured for up to 4 h are shown in Fig. 4. The plots for A549 and NHBE cells show similarity. Thus, the peak of response reported by ATM and Chk2 phosphorylation was between 1 and 2 h after exposure of either A549 or NHBE cells to CS. The steepest slope of Δ showing the *maximal rate* of increase of ATM and Chk2 phosphorylation was during the first hour after exposure, for both cell types. The maximal rate of increase in phosphorylation of H2AX was between the first and second hour, peaking at 2 h at a level 7.0 – 8.0 fold higher than the respective levels of the mock treated cells. The maximal rate of phosphorylation of p53 was during the first 2 h after exposure to CS, but the peak level was only two-fold higher than in the mock treated cells. The decline in expression of ATM-*Ser*1891^{P}, Chk2-*Thr*68^{P} and γH2AX, likely reporting their *dephosphorylation*, started to occur 2 h after exposure of A549 and NHBE cells to CS, reaching a nadir at 4 h. Dephosphorylation of p53-*Ser*15^{P} was seen in NHBE cells after 2 h but was not apparent in A549 cells.

There were differences in the response to CS vis-à-vis cell cycle phase (Fig. 4). Activation of ATM was most pronounced in S phase cells in both A549 and NHBE cells. Chk2 phosphorylation in NHBE cells was also more distinct in S than in G_1 or G_2M cells. This was not the case however in A549 cells that showed no clear differences in expression of Chk2-*Thr*68^{P} with regard to cell cycle phase. Phosphorylation of H2AX at the peak of response was most advanced in G_1 and S phase of A459 cells and in G_1 phase in NHBE cells. The cell cycle phase-dependent changes in the level of p53 phosphorylation were minimal. It should be noted that no significant differences in the cell cycle distribution (DNA content frequency histograms) were seen in A549 or NHBE cells after their exposure to CS for 20 min following their subsequent culturing for up to 4 h (Fig. 1 and Fig. 2).

Discussion

The DDR is a highly complex process involving the induction of a plethora of interactions between a variety of molecules engaged in DNA repair, controlling cell cycle progression, and associated with modulation of the cell's proclivity to undergo apoptosis (reviews, 28–34). One of earliest events of DDR is remodeling of chromatin that involves its decondensation also defined as relaxation (42–44). The relaxation increases the accessibility of the damaged DNA sites to the repair machinery. Translocation of the MRN complex consisting of Meiotic Recombination 11 Homolog A (Mre11), Rad50 homolog and Nijmegen Breakage Syndrome 1 (NMR1) into the damage site and activation of ATM protein kinase take place concurrent with chromatin decondensation (33,45,46). The activation of ATM seems to be triggered by chromatin decondensation and relaxation of the torsional stress of the DNA double helix upon induction of DNA damage (47). The MRN is essential in the process of ATM activation, since it recognizes DNA damage, recruits ATM to the damage site and also targets ATM to the respective substrates to initiate their phosphorylation (33,34). Activation of ATM occurs through autophosphorylation on *Ser*1981 and is preceded by acetylation that is mediated by the Tip60 histone acetyltransferase (48). It has been reported that upon induction of DNA damage by ionizing

radiation, activation ATM correlates strongly with the number of DSBs but not with the number of single-strand (ss) DNA breaks (SSBs) or other ss DNA lesions (49).

Among other substrates phosphorylated by ATM are p53 (TP53), checkpoint proteins Chk2 and Chk1, and H2AX (27,28,50) Activation of the checkpoint pathways results in arrest of progression though the cell cycle until the integrity to DNA is restored by the repair mechanisms. Checkpoint kinase 2 (Chk2) plays a key role in response of the cell cycle progression machinery to DNA damage (51) Activation of Chk2 mediated by ATM involves its phosphorylation on *Thr*68 which leads to Chk2 dimerization (50). In certain instances however, such as in response to replication stress, phosphorylation of Chk2 on Thr68 is mediated by ATR (50). Dimerization of Chk2 facilitates its intermolecular phosphorylation on *Thr*383, *Thr*387 and *Ser*516 which leads to dissociation of the dimers and formation of enzymatically active monomers. The enzymatically active dimers and monomers phosphorylate numerous substrates including Cdc25C and Cdc25A phosphatases. Phosphorylation of the Cdc25C and Cdc25A by Chk2 opens a binding site for 14-3-3 proteins, resulting in sequestration of the complex that, in turn, inhibits their translocation into the nucleus preventing dephosphorylation of *Thr*14 and *Tyr*15 on cyclin/CDK complexes, which stalls cell cycle progression at the G_2 to M transition or in G_1 phase, respectively (50).

Chk2 can also promote apoptosis in response to DNA damage. Activation of E2F-1 transcription factor provides one mechanism through which Chk2 increases the cell's proclivity to undergo apoptosis (52). Another mechanism is based on phosphorylation of the tumor suppressor protein p53 on *Ser*15 which may lead to upregulation of the proapoptotic protein Bax. Phosphorylation of p53 can also lead to upregulation of $p21^{Waf1}$ thereby providing an additional mechanism to arrest cells in G_1 (53). Chk2 also stabilizes the FoxM1 transcription factor and thereby stimulates expression of DNA repair genes (54). Chk1 and Chk2 are redundant in their activities. There is also a significant redundancy between all three isoforms of Cdc25 proteases (Cdc25A, Cdc25B and Cdc25C) (55).

One of the proteins whose phosphorylation is critical for DNA repair is histone H2AX (32,56). Although H2AX can be phosphorylated by ATR and DNA-PKcs (54,55) there is strong evidence that when its phosphorylation is mediated by ATM, and particularly when it is immunocytochemically detected by the presence of distinct γH2AX foci, it reports the induction of DSBs (30,31,34,45,59,60).

In the present study we observed that exposure to CS triggered the critical phosphorylation of ATM, Chk2, H2AX and p53 activating all these DNA damage responders. The response was dependent on the length of exposure to CS. Since the concentration of smoke was constant in the exposure chamber, the *duration* of the exposure can be considered a surrogate for the *dose* of the genotoxic agents in CS taken up by the cells. The plots in Fig. 3 show a lag of about five minutes and then nearly linear time (dose)-dependence between exposure and activation of DDR proteins during the subsequent 5 to 20 min. The observed lag in phosphorylation of these proteins during the initial five minutes most likely reflects (i) the time of penetration of the genotoxic substances in CS through the thin layer of PBS overlying the cells, the plasma membrane and the cytoplasmic compartment overlying the nucleus until they reach nuclear DNA and initiate the damage, and (ii) the ability of membrane permeable CS components to generate genotoxic free radicals within the cell. However, after the 5 min lag period, the smoke-dose-dependence of DDR of both A549 and NHBE cells was evident (Fig. 3).

The kinetics of phosphorylation of ATM, Chk2 and H2AX during the initial 1–2 h after exposure to smoke was similar in both A549 and NHBE cells (Fig. 4). Also similar in both

cell types was a decline in the level of phosphorylation of ATM-*Ser*1981^P, Chk2-*Thr*68^P and γH2AX, reflecting their dephosphorylation, observed between 2 h and 4 h. The decline was very pronounced and, after 4 h, the level of phosphorylation of these proteins was several-fold lower than at the peak of response. The only difference between A549 and NHBE cells in the kinetics was dephosphorylation of p53-*Ser*15^P which 4 h after exposure to CS remained phosphorylated in A549 cells but underwent partial dephosphorylation in NHBE cells. Since dephosphorylation of these proteins is considered to represent completion of the repair and disengagement of the checkpoints allowing the cells to resume the cell cycle progression (61,62) our data suggest this process occurred at similar rates in A549 and NHBE cells. There is a discrepancy in the literature as to whether protein phosphatase 2A (PP2A) (61) or PP4 (63) is the key phosphatase that dephosphorylates γH2AX.

The cell cycle phase dependent differences in response to CS were evident, particularly in A549 cells. Analysis of the raw data clearly indicates that phosphorylation of ATM, Chk2 and H2AX was more pronounced during S phase than during G_1 or G_2M (Fig. 1). This is reflected by the distinct “horseshoe” shape of the bivariate DNA versus IF distributions. Phosphorylation of H2AX was also more extensive in S phase of NHBE cells (Fig. 2). However, the plots presenting the mean values of IF of G_1 S or G_2M cell populations either as a function of an increase in time of exposure to CS (“dose” of CS) (Fig. 3) or the kinetics of DDR (Fig. 4) do not show such distinct cell cycle phase differences. This can be explained by the fact that among the gated G_1 or G_2M cells were the cells that during the time of exposure to smoke and subsequent incubation were either entering S or G_2 phase and though exposed during DNA replication when harvested had a DNA content close to that of G_1 or G_2M cells. The gating analysis based on DNA content of the cells represented by the characteristic pattern of “horseshoe” bivariate distributions, such as those incorporating BrdU, includes into the G_1 and G_2 populations the cells that during the exposure to BrdU (64), or in the present case, during treatment with smoke and subsequent incubation, were *entering* S and G_2.

Among A549 cells at the peak of expression (2 h), populations of G_1 and S cells had the highest levels of γH2AX (Fig. 4). In contrast, the S-phase NHBE cells showed much less of an increase of γH2AX expression than G_1 cells. This reflects the fact that consistent with our earlier observations (38,41,65) the control (mock treated) S phase NHBE cells had exceptionally high level of γH2AX, much higher than S phase A549 cells. Thus, although the total level of γH2AX in S phase cells after CS treatment was similar in A549 (Fig. 1) and NHBE cells (Fig. 2) the increase (Δ) when expressed as an *n-fold rise above the control S-phase cells* was more pronounced in A549 than in NHBE cells.

The degree of response to CS in terms on n-fold increase in phosphorylation was distinctly lower for p53 than for H2AX, ATM or Chk2. It is possible that this relatively low increase in expression of p53-*Ser*15 was already fully adequate for its effective signaling along the DDR pathway. It is also possible, however, that the phospho-specific Ab directed toward the p53-*Ser*15 epitope was less effective to detect the phosphorylation.

Assessment of DDR induced by exposure of normal (NHBE) or tumor (A549) cells to CS using phospho-specific Ab to detect critical phosphorylations of the responding molecules and measuring the response by LSC provides important information about the genotoxicity of mainstream CS. It was recently reported however, that exposure of A549 cells to sidestream smoke also induces H2AX phosphorylation (66). Of importance is the present observation that the response of A549 cells to CS was essentially similar to that of NHBE cells. This finding provides justification for the use of A549 cells in assessment of genotoxicity of CS in lieu of normal bronchial epithelial cells. Use of the latter cells is more

costly and complex because of the necessity to grow them in specially formulated media and within a restricted number of generations. Standardization of these normal cells may also be problematic due to variability of age, gender and other factors (e.g. including smoking status) of the cells' donor, as well as of variable number of generations in culture.

The induction of DSBs by exposure to CS was greater in S-phase than in G_1 or G_2M phase cells. Thus, our present data are consistent with the mechanism in which CS may initially generate ssDNA lesions and the collisions of replication forks during S-phase transform these lesions into DSBs. Among the ssDNA lesions induced by CS, the predominant ones are most likely oxidation-induced products such as adducts to DNA nucleobases including 8-hydroxy-2'-deoxyguanosine, the latter considered a biomarker for carcinogenesis (67,68). Indeed, the induction of γH2AX whether by mainstream- (26) or sidestream-CS (66) is to a large extent prevented by the oxidant scavenger N-acetylcysteine. Furthermore, the overall pattern of DDR after induction of oxidative DNA damage by H_2O_2 as detected by ATM, H2AX, Chk2 and p53 phosphorylation in A549 cells and measured by cytometry (69) was similar to the presently seen in CS treated cells.

Fully functional DDR is a critical anti-cancer barrier preventing the cell from undergoing genetic instability and malignant conversion. Cells can breach this barrier and undergo malignant progression if there are complementary mutations or other defects in key genes within this pathway (*e.g.*, p53, Chk2, ATM, etc.). Evidence to support the plausibility of this model in lung cancer is shown by the fact that: (i) p53 mutations are among the most common genetic defects in lung cancer (70,71); (ii) due to promoter methylation, Chk2 kinase expression is down-regulated in non-small cell lung carcinoma (72); and (iii) a significant reduction in DSB repair capacity is associated with increased promoter methylation of specific DDR genes which, in turn, is associated with an elevated risk of lung cancer (73). Collectively, these data suggest that one of the potentially pivotal carcinogenic DNA defects caused by CS is the induction of DNA damage in the form of DSBs.

Acknowledgments

Supported in part by NCI grant R01 28704.

Grant sponsor: NCI; Grant number CA 28 704

Literature cited

1. Hecht SS. Tobacco carcinogens, their biomarkers and tobacco-induced cancer. Nature Reviews: Cancer. 2003; 3:733–744.
2. Vineis P, Alavanja M, Buffler P, Fontham E, Franceschi S, Gao YT, Gupta PC, Hackshaw A, Matos E, Samet J, Sitas F, Smith J, Stayner L, Straif K, Thun MJ, Wichmann HE, Wu AH, Zaridze D, Peto R, Doll R. Tobacco and cancer: recent epidemiological evidence. J Natl Cancer Inst 2004. 2004; 96:99–106.
3. Rubin H. Synergistic mechanisms in carcinogenesis by polycyclic aromatic hydrocarbons and by tobacco smoke: a bio-historical perspective with updates. Carcinogenesis. 2001; 22:1903–1930. [PubMed: 11751421]
4. DeMarini DM. Genotoxicity of tobacco smoke and tobacco smoke condensate: a review. Mutat Res. 2004; 567:447–474. [PubMed: 15572290]
5. Fowles J, Dybing E. Application of toxicological risk assessment principles to the chemical constituents of cigarette smoke. Tob Control. 2003; 2:424–430. [PubMed: 14660781]
6. Hoffman, D.; Hecht, SS. Advances in tobacco carcinogenesis. In: Cooper, CS.; Grover, PL., editors. Handbook of Experimental Pharmacology. Heidelberg: Springer-Verlag; 1990. p. 63-102.

7. International Agency for Research on Cancer. IARC. Monographs on the Evaluation of Carcinogenic Risks to Humans. Vol. Vol 83. Lyon, FR: IARC; 2004. p. 1012-1065.Tobacco Smoke and Involuntary Smoking;
8. Hecht SS. Progress and challenges in selected areas of tobacco carcinogenesis. Chem Res Toxicol. 2008; 21:160–171. [PubMed: 18052103]
9. Hatsukami DK, Benowitz NL, Rennard SI, Oncken C, Hecht SS. Biomarkers to assess the utility of potential reduced exposure tobacco products. Nicot Tob Res. 2006; 8:600–622.
10. Kim TM, Yim SH, Lee JS, Kwon MS, Ryu JW, Kang HM, Fiegler H, Carter NP, Chung YJ. Genome-wide screening of genomic alterations and their clinico-pathologic implications in non-small cell lung cancers. Clin Cancer Res. 2005; 11:8235–8242. [PubMed: 16322280]
11. Laugesen M, Fowles J. Scope for regulation of cigarette smoke toxicity according to brand differences in toxicant emissions. N Z Med J. 2005; 118:U1401. [PubMed: 15843830]
12. Pankow JF. A consideration of the role of gas/particle partitioning in the deposition of nicotine and other tobacco smoke compounds in the respiratory tract. Chem Res Toxicol. 2001; 4:1465–1481. [PubMed: 11712903]
13. Franklin WA, Gazdar AF, Haney J, Wistuba II, La Rosa FG, Kennedy T, Ritchey DM, Miller YE. Widely dispersed p53 mutation in respiratory epithelium. A novel mechanism for field carcinogenesis. J Clin Invest. 1997; 100:2133–2137. [PubMed: 9329980]
14. Fujii T, Dracheva T, Player A, Chacko S, Clifford R, Strausberg RL, Buetow K, Azumi N, Travis WD, Jen J. A preliminary transcriptome map of non-small cell lung cancer. Cancer Res. 2002; 62:3340–3346. [PubMed: 12067970]
15. Guo M, House MG, Hooker C, Han Y, Heath E, Gabrielson E, Yang SC, Baylin SB, Herman JG, Brock MV. Promoter hypermethylation of resected bronchial margins: a field defect of changes? Clin Cancer Res. 2004; 10:5131–5136. [PubMed: 15297416]
16. Minna JD, Fong K, Zochbauer-Muller S, Gazdar AF. Molecular pathogenesis of lung cancer and potential translational applications. Cancer J. 2002; 8(Suppl 1):S41–S46. [PubMed: 12075701]
17. Sikkink SK, Liloglou T, Maloney P, Gosney JR, Field JK. In-depth analysis of molecular alterations within normal and tumour tissue from an entire bronchial tree. Int J Oncol. 2003; 22:589–595. [PubMed: 12579312]
18. Godtfredsen NS, Prescott E, Osler M. Effect of smoking reduction on lung cancer risk. JAMA. 2005; 294:1505–1510. [PubMed: 16189363]
19. Kiyohara C, Takayama K, Nakanishi Y. Association of genetic polymorphisms in the base excision repair pathway with lung cancer risk: a meta-analysis. Lung Cancer. 2006:54267–54283.
20. Wu X, Gu J, Spitz MR. Mutagen sensitivity: a genetic predisposition factor for cancer. Cancer Res. 2007; 67:3493–3495. [PubMed: 17440053]
21. Elliott B, Jasin M. Double-strand breaks and translocations in cancer. Cell Mol Life Sci. 2002; 59:373–385. [PubMed: 11915950]
22. Masuda A, Takahashi T. Chromosome instability in human lung cancers: possible underlying mechanisms and potential consequences in the pathogenesis. Oncogene. 2002; 21:6884–6897. [PubMed: 12362271]
23. Mills KD, Ferguson DO, Alt FW. The role of DNA breaks in genomic instability and tumorigenesis. Immunol Rev. 2003; 194:77–95. [PubMed: 12846809]
24. Sekido Y, Fong KM, Minna JD. Molecular genetics of lung cancer. Annu Rev Med. 2003; 54:73–87. [PubMed: 12471176]
25. Albino AP, Huang X, Yang J, Gietl D, Jorgensen E, Traganos F, Darzynkiewicz Z. Induction of histone H2AX phosphorylation in A549 human pulmonary epithelial cells by tobacco smoke and in human bronchial epithelial cells by smoke condensate: A new assay to detect the presence of potential carcinogens in tobacco. Cell Cycle. 2004; 3:1062–1068. [PubMed: 15254392]
26. Albino AP, Huang X, Jorgensen E, Gietl D, Traganos F, Darzynkiewicz Z. Induction of DNA double-strand breaks in A549 and normal human pulmonary epithelial cells by cigarette smoke is mediated by free radicals. Int J Oncol. 2006; 28:1491–1505. [PubMed: 16685450]
27. Tanaka T, Huang X, Jorgensen E, Gietl E, Traganos F, Darzynkiewicz Z, Albino AP. ATM activation accompanies histone H2AX phosphorylation in A549 cells upon exposure to tobacco smoke. BMC Cell Biol. 2007:8–26. Epub June 26. [PubMed: 17326840]

28. Kastan MB, Lim DS. The many substrates and functions of ATM. Nat Rev Mol Cell Biol. 2000; 1:179–186. [PubMed: 11252893]
29. Helt CE, Cliby WA, Keng PC, Bambara RA, O'Reilly MA. Ataxia telangiectasia mutated (ATM) and ATM and Rad3-related protein exhibit selective target specificities in response to different forms of DNA damage. J Biol Chem. 2005; 280:1186–1192. [PubMed: 15533933]
30. Bakkenist CJ, Kastan MB. DNA damage activates ATM through intermolecular autophosphorylation and dimer dissociation. Nature. 2003; 421:499–506. [PubMed: 12556884]
31. Bakkenist CJ, Kastan MB. Initiating cellular stress responses. Cell. 2004; 118:9–17. [PubMed: 15242640]
32. Burma S, Chen BP, Murphy M, Kurimasa A, Chen DJ. ATM phosphorylates histone H2AX in response to DNA double-strand breaks. J Biol Chem. 2001; 276:42462–42467. [PubMed: 11571274]
33. Lee J-H, Paull TT. ATM activation by DNA double-strand breaks through the Mre11-Rad50-Nbs1 complex. Science. 2005; 308:551–554. [PubMed: 15790808]
34. Paull TT, Lee JH. The Mre11/Rad50/Nbs1 complex and its role as a DNA-double strand break sensor for ATM. Cell Cycle. 2005; 4:737–740. [PubMed: 15908798]
35. Zhao H, Traganos F, Darzynkiewicz Z. Phosphorylation of p53 on *Ser*15 during cell cycle caused by Topo I and Topo II inhibitors in relation to ATM and Chk2 activation. Cell Cycle. 2008; 7:3048–3055. [PubMed: 18802408]
36. Zhao H, Traganos F, Albino AP, Darzynkiewicz Z. Oxidative stress induces cell cycle- dependent Mre11 recruitment, ATM and Chk2 activation and histone H2AX phosphorylation. Cell Cycle. 2008; 7:1490–1495. [PubMed: 18418078]
37. Zhao H, Traganos F, Darzynkiewicz Z. Kinetics of histone H2AX phosphorylation and Chk2 activation in A549 cells treated with topotecan and mitoxantrone in relation to the cell cycle phase. Cytometry A. 2008; 73A:480–489. [PubMed: 18459160]
38. Zhao H, Tanaka T, Halicka HD, Traganos F, Zarebski M, Dobrucki J, Darzynkiewicz Z. Cytometric assessment of DNA damage by exogenous and endogenous oxidants reports the aging-related processes. Cytometry A. 2007; 71A:905–914. [PubMed: 17879239]
39. Pozarowski P, Holden E, Darzynkiewicz Z. Laser scanning cytometry. Principles and applications. Meth Molec Biol. 2005; 319:165–192.
40. Darzynkiewicz Z, Bedner E, Gorczyca W, Melamed MR. Laser scanning cytometry. A new instrumentation with many applications. Exp Cell Res. 1999; 249:1–12. [PubMed: 10328948]
41. Tanaka T, Halicka HD, Huang X, Traganos F, Darzynkiewicz Z. Constitutive histone H2AX phosphorylation and ATM activation, the reporters of DNA damage by endogenous oxidants. Cell Cycle. 2006; 5:1940–1945. [PubMed: 16940754]
42. Murga M, Jaco I, Soria R, Martinez-Pastor B, Cuadrado M, Yang S-M, Blasco MA, Skoultchi AI, Fernandez-Capetillo O. Global chromatin compaction limiCS the strength of the DNA damage response. J Cell Biol. 2007; 178:1101–1108. [PubMed: 17893239]
43. Gerlitz G, Hock R, Ueda T, Bustin M. The dynamics of HMG protein-chromatin interactions in living cells. Biochem Cell Biol. 2009; 87:127–137. [PubMed: 19234529]
44. Halicka HD, Zhao H, Podhorecka M, Traganos F, Darzynkiewicz Z. Cytometric detection of chromatin relaxation, an early reporter of DNA damage response. Cell Cycle. (in press).
45. Abraham RT, Tibbetts RS. Guiding ATM to broken DNA. Science. 2005; 308:510–511. [PubMed: 15845843]
46. Downs JA, Cote J. Dynamics of chromatin during the repair of DNA doublestrand breaks. Cell Cycle. 2005; 4:1373–1376. [PubMed: 16205111]
47. Kitagawa R, Kastan MB. The ATM-dependent DNA damage signaling pathway. Cold Spring Harb Symp Quant Biol. 2005; 70:99–109. [PubMed: 16869743]
48. Sun Y, Jiang X, Chen S, Fernandes N, Price BD. A role for the Tip60 histone acetyltransferase in the acetylation and activation of ATM. Proc Natl Acad Sci USA. 2005; 102:13182–13187. [PubMed: 16141325]
49. Ismail IH, Nystrom S, Nygren J, Hammersten O. Activation of ataxia telangiectasia mutated by DNA strand break-inducing agents correlates closely with the number of DNA double strand breaks. J Biol Chem. 2005; 280:4649–4655. [PubMed: 15546858]

50. Ahn J, Urist M, Prives C. The Chk2 protein kinase. DNA Repair. 2004; 3:1039–1047. [PubMed: 15279791]
51. Matsuoka S, Rotman G, Ogawa A, Shiloh K, Tamai SJ, Elledge SJ. Ataxia telangiectasia-mutated phosphorylates Chk2 in vivo and in vitro. Proc Natl Acad Sci USA. 2000; 97:10289–10394.
52. Stevens C, Smith L, La Thangue NB. Chk2 activates E2F-1 in response to DNA damage. Nat Cell Biol. 2003; 5:4465–4479.
53. Lin J, Reichner C, Wu X, Levine AJ. Analysis of wild-type and mutant p21WAF-1 gene activities. Mol Cell Biol. 1996; 16:86–1793. [PubMed: 8524332]
54. Tan Y, Raychaudhuri P, Costa RH. Chk2 mediates stabilization of the FoxM1 transcription factor to stimulate expression of DNA repair genes. Mol Cell Biol. 2007; 27:1007–1016. [PubMed: 17101782]
55. Rudolph J. Cdc25 phosphatases: Structure, specificity and mechanism. Biochemistry. 2007; 46:3595–3604. [PubMed: 17328562]
56. Sedelnikova OA, Rogakou EP, Panuytin IG, Bonner W. Quantitative detection of ^{125}IUdr-induced DNA double-strand breaks with γ-H2AX antibody. Radiation Res. 2002; 158:486–492. [PubMed: 12236816]
57. Stiff TO, Driscoll M, Rief N, Iwabuchi K, Lobrich M, Jeggo PA. ATM and DNA-PK function redundantly to phosphorylated H2AX after exposure to ionizing radiation. Cancer Res. 2004; 64:2390–2396. [PubMed: 15059890]
58. Wang H, Wang M, Wang H, Bocker W, Illiakis G. Complex H2AX phosphorylation patterns by multiple kinases including ATM and DNA-PK in human cells exposed to ionizing radiation and treated with kinase inhibitors. J Cell Phys. 2005; 202:492–502.
59. Bonner WM, Redon CE, Dickey JS, Nakamura AJ, Sedelnikova OA, Solier S, Pommier Y. γH2AX and cancer. Nat Reviews. 2008; 8:957–967.
60. Bartkova J, Bakkenist CJ, Rajpert-De Meyts E, Skakkebaek NE, Sehested M, Lukas J, Kastan MB, Bartek J. ATM activation in normal human tissues and testicular cancer. Cell Cycle. 2005; 4:838–845. [PubMed: 15846060]
61. Chowdhury D, Keogh MC, Ishii H, Peterson CL, Buratowski S, Lieberman J. gamma-H2AX dephosphorylation by protein phosphatase 2A facilitates DNA double-strand break repair. Mol Cell. 2005; 20:801–809. [PubMed: 16310392]
62. Heideker J, Lis ET, Romesberg FE. Phosphatases, DNA damage checkpoints and checkpoint deactivation. Cell Cycle. 2007; 6:3058–3064. [PubMed: 18075314]
63. Nakada S, Chen GI, Gingras AC, Darocher D. PP4 is a gamma H2AX phosphatase required for recovery from DNA damage checkpoint. EMBO Rep. 2008; 9:1019–1026. [PubMed: 18758438]
64. Juan G, Li X, Darzynkiewicz Z. Correlation between DNA replication and expression of cyclins A and B1 in individual MOLT-4 cells. Cancer Res. 1997; 57:803–807. [PubMed: 9041174]
65. Huang X, Tanaka T, Kurose A, Traganos F, Darzynkiewicz Z. Constitutive histone H2AX phosphorylation on *Ser*-139 in cells untreated by genotoxic agents is cell-cycle phase specific and attenuated by scavenging reactive oxygen species. Int J Oncol. 2006; 29:495–501. [PubMed: 16820894]
66. Toyooka T, Ibuki Y. Cigarette sidestream smoke induces phosphorylated histone H2AX. Mutat Res. 2009; 676:34–40. [PubMed: 19486862]
67. Valavanidis A, Vlachogianni T, Fiotakis K. Tobacco Smoke: Involvement of reactive oxygen species and stable free radicals in mechanisms of oxidative damage, carcinogenesis and synergistic effects with other respirable particles. Int J Environ Res Public Health. 2009; 6:445–462. [PubMed: 19440393]
68. Asami S, Manabe H, Miyake J, Tsurudone Y, Hirano T. Cigarette smoking induces an increase in oxidative DNA damage, 8-hydroxydeoxyguanosine, in a central site of human lung. Carcinogenesis. 1997; 18:1763–1766. [PubMed: 9328173]
69. Zhao H, Traganos F, Albino AP, Darzynkiewicz Z. Oxidative stress induces cell cycle-dependent Mre11 recruitment, ATM and Chk2 activation and histone H2AX phosphorylation. Cell Cycle. 2008; 7:1490–1495. [PubMed: 18418078]
70. Robles AI, Linke SP, Harris CC. The p53 network in lung carcinogenesis. Oncogene. 2002; 21:6898–6907. [PubMed: 12362272]

71. Pfeifer GP, Hainaut P. On the origin of G -->T transversions in lung cancer. Mutat Res. 2003; 526:39–43. [PubMed: 12714181]

72. Zhang P, Wang J, Gao, Yuan BZ, Rogers J, Reed E. CHK2 kinase expression is down-regulated due to promoter methylation in non-small lung cancer. Molec Cancer. 2004; 3:14. (1–10). [PubMed: 15125777]

73. Leng S, Stidley CA, Willink R, Bernauer A, Do K, Picchi MA, Sheng X, Frasco MA, Van Den Berg D, Gilliland FD, Zima C, Crowell RE, Belinsky SA. Double-strand break damage and associated DNA repair genes predispose smokers to gene methylation. Cancer Res. 2008; 68:3049–3056. [PubMed: 18413776]

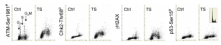

Fig. 1. Effect of exposure of A549 cells to CS on expression of ATM-*Ser*1981^{P}, Chk2-*Thr*68^{P}, γH2AX and p53-*Ser*15^{P}

The cells were exposed for 15 min to CS from 2R4F cigarette then transferred to a CO_2 incubator and cultured for 1 h. The induction of ATM-*Ser*1981^{P}, Chk2-*Thr*68^{P}, γH2AX and p53-*Ser*15^{P} was detected immunocytochemically and measured by LSC, in conjunction with cellular DNA content, as described in Materials and Methods. Mock-treated cells served as a control. The DNA content frequency histogram of the CS-treated cells from the representative culture is shown in the right panel; control cells had nearly identical histograms (not shown).

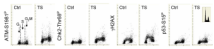

Fig. 2. Expression of ATM-*Ser*1981^{P}, Chk2-*Thr*68^{P}, γH2AX and p53-*Ser*15^{P} in NHBE cells mock-treated (Ctrl) or exposed to CS

The cells were treated with CS for 15 min then cultured for 1 h prior to fixation. As in Fig. 1 the DNA content frequency histogram of a representative culture is shown (right panel)

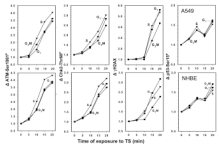

Fig. 3. Effect of length of cells exposure to CS on the increase (Δ) in expression of ATM-*Ser*1981^{P}, Chk2-*Thr*68^{P}, γH2AX and p53-*Ser*15^{P}

A549 cells (top panels) and NHBE cells (bottom panels) were exposed to CS as described in Materials and Methods for periods of 5 – 20 min and then were transferred to culture for 1 h before being harvested and fixed. The mean values of ATM-*Ser*1981^{P}, Chk2-*Thr*68^{P}, γH2AX and p53-Ser15^{P} immunofluorescence were measured for populations of cells in G_1, S and G_2M phases of the cell cycle by gating analysis based on differences in DNA content. The data are expressed as the n-fold increase of these mean values (Δ) over the respective values of the mock-treated cells.

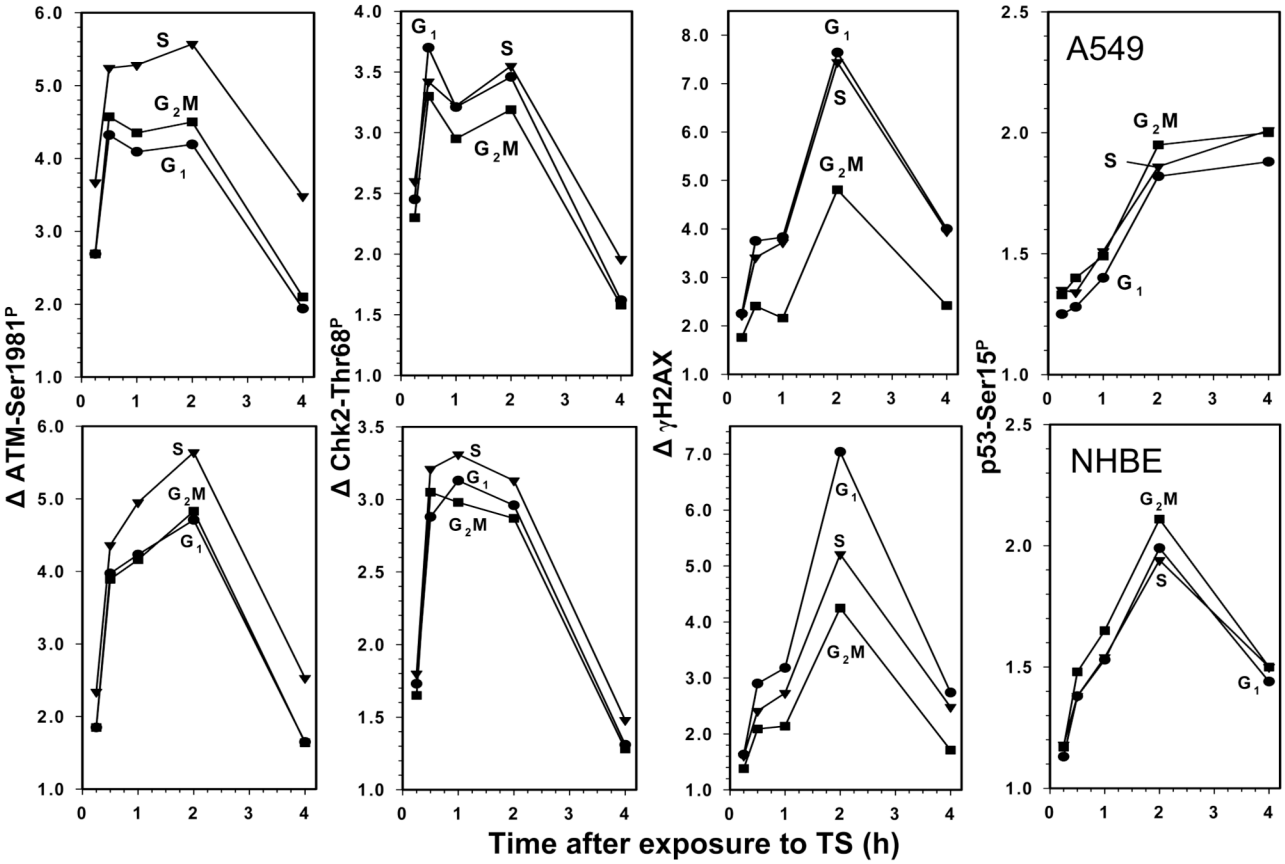

Fig. 4. Effect of duration of cell culturing after their exposure to CS on the expression of ATM-*Ser*1981^P, Chk2-*Thr*68^P, γH2AX and p53-*Ser*15^P

A549 cells (top panels) or NHBE cells (bottom panels) were treated with CS for 20 min, then transferred into culture and grown for 0.25 h, 0.5 h, 1 h, 2 h, and 4 h before the cultures were terminated. The mean values of ATM-*Ser*1981^P, Chk2-*Thr*68^P, γH2AX and p53-*Ser*15^P immunofluorescence were estimated for populations of G_1, S and G_2M-phase cells. The data are expressed as the n-fold increase of these mean values (Δ) over the respective values of the mock-treated cells.